Acta Crystallographica Section D
Biological Crystallography
ISSN 0907-4449

Structure determination of bacterioferritin from *Desulfovibrio desulfuricans* by the MAD method at the Fe *K*-edge

Ana V. Coelho,[a,b] Sofia Macedo,[a] Pedro M. Matias,[a] Andrew W. Thompson,[c] Jean LeGall[a,d] and Maria Arménia Carrondo[a]*

[a]Instituto de Tecnologia Química e Biológica, Universidade Nova de Lisboa, Av. da República, EAN, Apartado 127, 2781-901 Oeiras, Portugal, [b]Chemistry Department, Universidade de Évora, Apartado 94, 7001 Évora Codex, Portugal, [c]EMBL Grenoble Outstation, c/o ILL 20, BP-156, F-38042 Grenoble CEDEX, France, and [d]Department of Biochemistry and Molecular Biology, University of Georgia, Athens, GA 30602, USA

Correspondence e-mail: carrondo@itqb.unl.pt

Received 23 August 2000
Accepted 25 October 2000

Bacterioferritins constitute a subfamily of heme ferritins, proteins involved in iron storage and homeostasis. The protein isolated from *Desulfovibrio desulfuricans* ATCC 27774 is a homodimer of mass 52 kDa. The monomers are linked by an iron-coproporphyrin group and each monomer contains a diferric center. The 24-monomer clusters found in the crystal are probably the functional particles. MAD data from cubic bacterioferritin crystals were collected at the *K*-shell iron edge. Preliminary phasing was performed using the positions of 23 of the 40 Fe atoms expected in the asymmetric unit. Further MAD phasing allowed the identification of individual iron sites. Clear and interpretable electron-density maps were obtained after density modification.

1. Introduction

Ferritins are omnipresent as iron-storage proteins in living organisms and appear to play a central role in iron homeostasis. A subfamily of these proteins, called bacterioferritins, differs from the mammalian-type ferritins in terms of amino-acid sequence, immunological cross-reactivity, composition of the iron core and by the presence of a heme group (Harrison & Arosio, 1996; Andrews, 1998). Very recently, a new bacterioferritin has been found in the sulfate-reducing bacterium *Desulfovibrio desulfuricans* strain ATCC 27774 grown with nitrate as the terminal electron acceptor. Although spectroscopic analysis suggests the presence of di-iron centers and its primary structure shows clear homologies with previously described bacterioferritins, this new protein is unique in the sense that it does not contain iron-porphyrin IX (Romão, Regalla *et al.*, 2000) but rather an iron-coproporphyrin group (Romão, Louro *et al.*, 2000).

Like all other sulfate-reducing bacteria, the ATCC 27774 *Desulfovibrio* strain is capable of growing using sulfate as the terminal electron acceptor and can also make the same use of nitrate, which is reduced to ammonia. These bacteria are well known for their detrimental activity; they are the origin of the corrosion of iron (Hamilton & Lee, 1995). They are also opportunistic pathogens, as some ATCC 27774 related strains have recently been shown to be present in the blood of human patients and domestic animals, where they compete for the host's iron (Loubinoux *et al.*, 2000; Shukla & Reed, 2000). Although these particularities point to the importance of the mechanisms of iron homeostasis in sulfate-reducing bacteria, very little is known concerning this aspect of their metabolism. Thus, finding a bacterioferritin in one of these bacteria constitutes the first step towards the elucidation of this mechanism. The determination of its three-dimensional structure is therefore of particular relevance.

2. Materials, methods and results

2.1. Crystallization and crystal flash-cooling

Bacterioferritin was crystallized at room temperature using the sitting-drop vapor-diffusion method. The crystals thus obtained are red and have a cubic shape.

The first crystals were grown in the presence of 2.0 *M* ammonium sulfate, with different buffers and pH varying from 4.6 to 8.5. Better crystals were obtained using as crystallization solution 2.0 *M* ammonium sulfate in 0.1 *M* acetate buffer at pH values ranging from 3.6 to 5.5 or in 0.1 *M* Tris–HCl in the pH range 7–9. Crystallization drops containing 2 µl of protein solution and an equal amount of reservoir solution were allowed to equilibrate against 500 µl of the reservoir solution. The protein solution (13 mg ml^{-1}) purified under anaerobic conditions contained 0.3 *M* K_2HPO_4 as a stabilizing agent. Crystals grew in 5–7 d to dimensions of about 0.3 × 0.3 × 0.3 mm. Crystallization assays were performed in both anaerobic and aerobic environments. No differences were observed between crystals obtained under both conditions.

Good cryoconditions were obtained adding glycerol [25%(*v*/*v*)] to the mother liquor. The mosaicity tends to increase with time when the crystals are immersed into the cryoprotecting solution. Thus, the shortest possible time was used, leading to a mosaicity of 0.5°, which is

Table 1
X-ray data-processing statistics.

Values in parentheses refer to the last resolution shell.

MAD data set	1.7400 Å (inflection λ_1)	1.7387 Å (peak λ_2)	0.9920 Å (remote λ_3)	0.9920 Å (remote λ_3)
Resolution range (Å)	30.0–2.80	30.0–2.90	30.0–2.80 (low resolution)	30.0–2.40 (high resolution)
No. measured	795843	918149	632259	1084442
No. unique	92910	84287	91778	147431
Completeness (%)	99.9 (99.8)	99.9 (99.9)	99.8 (99.6)	99.9 (99.7)
Multiplicity	8.5	10.5	6.8	7.4
No. Bijvoet pairs	88645	79581	88083	140760
Completeness (%)	99.7	100.0	99.8	99.8
$I/\sigma(I)$	27.0 (5.0)	31.1 (10.8)	25.8 (6.0)	15.5 (3.0)
$R_{\rm sym}$† (%)	8.9(29.1)	8.8 (23.5)	7.4 (18.3)	12.7 (55.3)
$R_{\rm anom}$‡ (%)	4.3 (17.5)	4.0 (7.6)	3.1 (11.5)	5.1 (24.7)

† $R_{\rm sym} = \sum_h \sum_i |I_i(h) - \langle I(h)\rangle| / \sum_h \sum_i I_i(h)$, where $I_i(h)$ is the ith measurement of independent intensity with mean value $\langle I(h)\rangle$. ‡ $R_{\rm anom} = \sum |\langle I^+\rangle - \langle I^-\rangle| / \sum (\langle I^+\rangle + \langle I^-\rangle)$, where $\langle I^+\rangle$ and $\langle I^-\rangle$ denote the mean intensity values of each mate in a Bijvoet pair.

comparable with the value of 0.3° obtained at room temperature.

2.2. Data collection and preliminary crystallographic characterization

Data for MAD phasing were collected at three different wavelengths using a MAR CCD detector at the ESRF beamline BM-14 (Grenoble, France) from a single crystal frozen at 100 K in a nitrogen-gas stream with a Oxford Cryosystems low-temperature device. A preliminary X-ray fluorescence spectrum of a bacterioferritin crystal near the *K*-shell iron edge was measured. This was used to select the monochromator settings for the inflection point (λ_1 = 1.7400 Å, the minimum for $\Delta f'$), the peak (λ_2 = 1.7387 Å, the maximum for $\Delta f''$) and a remote point (λ_3 = 0.992 Å). The diffraction images were processed and scaled using the programs *DENZO* and *SCALEPACK* (Otwinowski & Minor, 1997). The indexed intensities were merged and converted to structure factors using the *CCP*4 program suite (Collaborative Computational Project, Number 4, 1994) (*ROTAPREP*/*SCALA*/*TRUNCATE*). Data-processing statistics are summarized in Table 1.

In order to verify the possible presence of manganese in this structure, as attributed in the structure of *Escherichia coli* bacterioferritin (Frolow *et al.*, 1994; Dautant *et al.*, 1998), a second fluorescence scan was performed near its *K*-shell edge. However, no absorption edge was observed, indicating the absence of manganese as a second anomalous scatterer.

Bacterioferritin crystals belong to the cubic space group $P2_13$, with unit-cell parameter a = 225.3 Å. Unit-cell volume considerations led to the conclusion that there would be eight dimers in the asymmetric unit. Since each dimer (MW $\simeq$ 52 kDa) was expected from the *E. coli* structure to contain five Fe atoms (four from two diferric centres and one from one heme), this would lead to a total of 40 Fe atoms per asymmetric unit. The estimated volume per unit of molecular weight ($V_{\rm M}$) is 2.29 Å^3 Da^{-1}, with a corresponding solvent content of 46%. This is within the normal range observed for protein crystals (Matthews, 1968).

The self-rotation Patterson maps (Fig. 1) present 423 point-group symmetry, higher than that corresponding to the crystallographic point group 23 (the point group for the space group $P2_13$). These results indicate the presence of additional non-crystallographic symmetry axes, a twofold and a fourfold, consistent with the 24-monomer cluster. This arrangement had already been suggested for this protein (Romão *et al.*, 2000) and is common to other bacterioferritins and ferritins. This arrangement also implies the presence of threefold non-crystallographic axes, which on the self-rotation Patterson map coincide with the crystallographic ones. From the type of the monomeric arrangement forming the cluster and from the unit-cell parameters and symmetry operations of the space group, the presence of two times one third of a cluster within the asymmetric unit was inferred. These clusters are related by a translation vector of (0.44, 0.44, 0.44) in fractional coordinates and thus the crystal structure is almost body-centered cubic.

2.3. Structure determination using MAD phasing

Data sets collected at wavelengths λ_1 and λ_2 were scaled to data measured at λ_3 using the program *SCALEIT* from the *CCP*4 program suite (Collaborative Computational Project, Number 4, 1994). The *Shake&Bake* (*SnB*) program (Miller *et al.*, 1993, 1994) was used and managed to identify 23 of the 40 expected iron sites in the asymmetric unit, which corresponded to almost three positions per dimer, instead of five as expected. The best solution found by *SnB* was thought to be correct for two reasons: firstly, in the histogram distribution of the 1000 trials it appeared well isolated from the cluster of the remaining 'wrong' solutions; secondly, inspection of the peaks in the graphics interface of *SnB* revealed a number of pairs of sites separated by about 13 Å, the approximate distance between the di-Mn centre and the heme Fe atom in *E. coli* bacterioferritin (Frolow *et al.*, 1994; Dautant *et al.*, 1998). These sites correspond to most

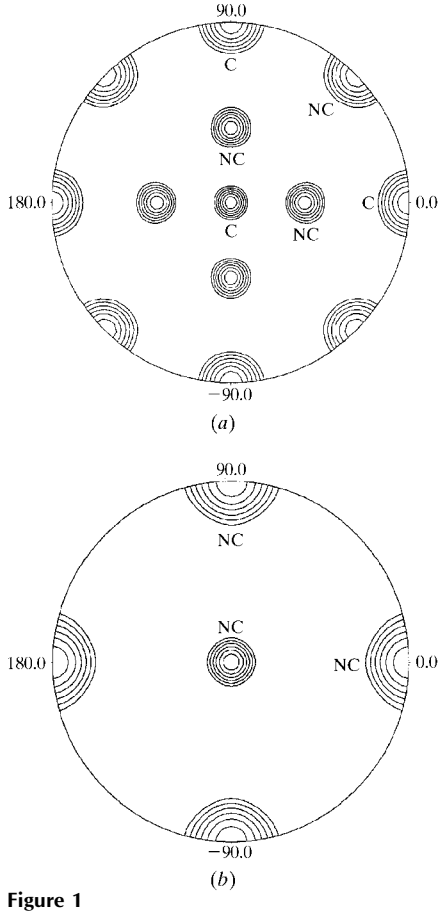

Figure 1
Self-rotation function plots for bacterioferritin crystals in the resolution range 4.5 < d < 20 Å with integration range 5 < R < 45 Å. Peaks in the sections shown at (*a*) κ = 180° and (*b*) κ = 90° give the orientation of the crystallographic twofold (C) and non-crystallographic twofold and fourfold (NC) rotation axes in the crystal structure. The maximum value was normalized to 100 and the contour drawn at 10-unit intervals, starting at 40. Drawings were prepared with the programs *NPO* and *XPLOT84-DRIVER* (Collaborative Computational Project, Number 4, 1994).

Table 2
MLPHARE phase-refinement statistics.

Wavelength	Phasing power†		$R_{\rm cullis}$‡		
	Centric	Acentric	Centric	Acentric	Anomalous
λ_1 (inflection)	—	—	—	—	0.84
λ_2 (peak)	0.30	0.48	0.95	0.95	0.83
λ_3 (remote low resolution)	0.73	1.15	0.78	0.79	0.95
λ_3 (remote high resolution)	0.60	0.90	0.81	0.82	0.97

† Phasing power = $\sum|F_H|/\sum\big||F_p(\lambda_a)|(\text{obs}) - |F_p(\lambda_a)|(\text{calc})\big|$, where F_H are Fe-atom structure factors and $F_p(\lambda_a)$ are protein structure factors observed (obs) and calculated (calc) at λ_a (λ_2, λ_3). ‡ $R_{\rm cullis} = \sum\big||F_p(\lambda_a)| - |F_p(\lambda_1)|\big| - |\Delta F_{\rm calc}|\big|\big/\sum\big||F_p(\lambda_a)| - |F_p(\lambda_1)|\big|$, where $F_p(\lambda_a)$ and $F_p(\lambda_1)$ are protein structure factors at λ_a (λ_2, λ_3) and λ_1, respectively. $\Delta F_{\rm calc}$ is the calculated dispersive difference between λ_a and λ_1. Summation was performed using centric and acentric reflections. $R_{\rm cullis\_anom} = \sum\big|\big||F_p^+(\lambda_a)| - |F_p^-(\lambda_a)|\big| - |\Delta F_{\rm calc}|\big|\big/\sum\big||F_p^+(\lambda_a)| - |F_p^-(\lambda_a)|\big|$, where $|F_p^+(\lambda_a)| - |F_p^-(\lambda_a)|$ is the Bijvoet difference at λ_a (λ_2, λ_3). $\Delta F_{\rm calc}$ is the calculated anomalous difference at λ_a.

of the peaks in the Patterson map calculated using the anomalous differences from the data set with highest anomalous signal (λ_2) as coefficients. In particular, a very large cluster of peaks was found at the fractional coordinates (0.44, 0.44, 0.44) which corresponds, as previously mentioned, to the translation vector between the two independent clusters of monomers in the unit cell. Because of the relatively weak anomalous signal, this Patterson map was rather noisy and so a perfect match between predicted and observed interatomic vectors could not be observed.

Phase refinement of these iron positions and MAD phasing were performed using the program *MLPHARE* (Collaborative Computational Project, Number 4, 1994). For the phasing procedure, the data set λ_1 was treated as a native data set with intrinsic anomalous scattering and the other two wavelengths were regarded as derivatives, following a procedure already described (Ramakrishnan *et al.*, 1993; Glover *et al.*, 1995). The preliminary phases were calculated and refined using data in the resolution range 15–2.7 Å. This process converged to an overall figure of merit of 0.54. Analysis of the *MLPHARE* results suggested that some of the sites found by *SnB* were in fact double sites. The impossibility of resolving these di-iron sites using the *SnB* protocol is explained by the low resolution of the diffraction data with anomalous signal (only to 2.9 Å, while the distance between the two sites in the di-iron centre was 3.4 Å) and also by the weak magnitude of the anomalous signal ($R_{\rm anom}$ was systematically below $R_{\rm merge}$ in all resolution shells). Thus, for some of the sites, an 'average' site per diferric center had been obtained. These possible 'averaged' di-Fe sites were identified by comparison with the metal sites in the *E. coli* bacterioferritin, which had a similar geometry. It was possible to resolve the di-Fe sites by leaving out in turn one of the possible 'averaged' di-Fe site from the *MLPHARE* refinement, carrying out a few cycles and looking at an anomalous Fourier map to identify the individual Fe-atom positions. The statistics for the phase calculation and refinement are presented in Table 2. Density-modification calculations (solvent flattening and histogram matching) and phase extension to 2.4 Å using the program *DM* (Collaborative Computational Project, Number 4, 1994) greatly improved the figure-of-merit value (0.81) and the overall aspect of the map (Fig. 2). Many α-helices are visible in the electron-density map.

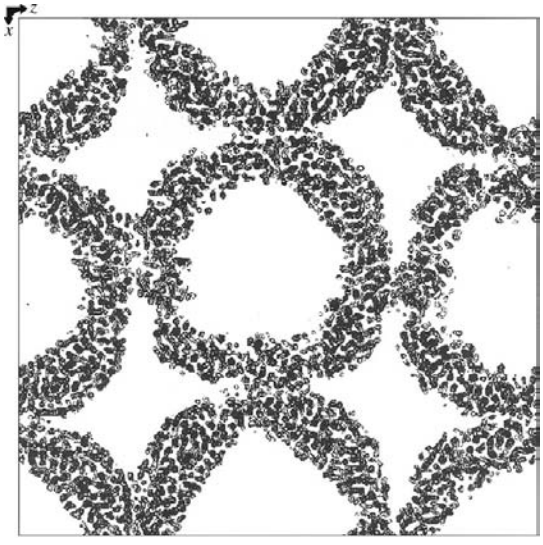

Figure 2
Superposition of ten electron-density map sections from a total of 114 calculated using the phases optimized by the program *DM* (Collaborative Computational Project, Number 4, 1994). The contours were drawn at 1.2σ unit intervals, starting at 1.2σ. Drawings were prepared with the programs *NPO* and *XPLOT84-DRIVER* (Collaborative Computational Project, Number 4, 1994).

3. Discussion

From the current results, it is possible to say with certainty that this bacterioferritin crystallizes as a 24-mer cluster containing 12 dimers with 24 di-iron centers and 12 heme groups, giving a total of 60 Fe atoms. In the unit cell there are eight of these clusters (two non-equivalent groups of four) located on crystallographic threefold axes (along the body diagonals of the cube). The remaining local symmetry elements of the 24-mer (twofold and fourfold axes) show up as non-crystallographic axes on a self-rotation Patterson map and will be used advantageously in the density-modification calculations. A puzzle that remains to be explained is why the structure of *D. desulfuricans* bacterioferritin could not be solved by the molecular-replacement method using the structure of *E. coli* bacterioferritin as a model. The size of both clusters seems to be about the same and the sequence homology between the two molecules is almost 50%. One possible explanation could be that since there are eight dimers in the asymmetric unit and since the molecular-replacement procedure in this case consists of the correct sequential placement of these dimers in the unit cell, it may be that only one dimer was not enough to provide a sufficiently clear starting solution for the procedure.

Another puzzle for the crystallographer is why the crystal structure is not body-centered. This may result from dimerization of the 24-monomer clusters in the unit cell, thus making the two independent 1/3 clusters non-equivalent.

Model building and structure refinement are presently under way.

The authors would like to thank the fermentation plant at the University of Georgia, Athens, GA, USA for growing the bacteria, M.-Y. Liu (UGA), Célia Romão and Isabel Pacheco (ITQB-UNL) for the purified protein samples used in these studies and ESRF for support with data collection. The work was supported by NIH grant GM56000-03 to JLG. JLG received a grant from PRAXIS XXI.

References

Andrews, S. (1998). *Adv. Microbial. Physiol.* **40**, 281–351.
Collaborative Computational Project, Number 4 (1994). *Acta Cryst.* D**50**, 760–763.
Dautant, A., Meyer, J. B., Yariv, J., Précigoux, G., Sweet, R. M., Kalb (Gilboa), A. J. & Frolow, F. (1998). *Acta Cryst.* D**54**, 16–24.
Frolow, F., Kalb (Gilboa), A. J. & Yariv, J. (1994). *Nature Struct. Biol.* **1**, 453–460.

Glover, I. D., Denny, R. C., Nguti, N. D., McSweeney, S. M., Kinder, S. H., Thompson, A. W., Dodson, E. J. & Tame, J. R. H. (1995). *Acta Cryst.* D**51**, 39–47.
Hamilton, W. A. & Lee, W. (1995). *Biocorrosion in Sulfate-Reducing Bacteria. Biotechnology Handbooks*, edited by L. L. Barton, Vol. 8, pp. 243–264. New York: Plenum Press.
Harrison, P. M. & Arosio, P. (1996). *Biophys. Biochem. Acta*, **1275**, 161–203.
Loubinoux, J., Mory, F., Pereira, I. A. C. & Le Faou, A. E. (2000). *J. Clin. Microbiol.* **38**, 931–934.
Matthews, B. W. (1968). *J. Mol. Biol.* **33**, 491–497.
Miller, R., DeTitta, G. T., Jones, R., Langs, D. A., Weeks, C. M. & Hauptman, H. (1993). *Science*, **259**, 1430–1433.
Miller, R., Gallo, S., Khalak, H. G. & Weeks, C. M. (1994). *J. Appl. Cryst.*, **27**, 613–621.
Otwinowski, Z. & Minor, W. (1997). *Methods Enzymol.* **276**, 307–326.
Ramakrishnan, V., Finch, J. T., Graziano, V., Lee, P. L. & Sweet, R. M. (1993). *Nature (London)*, **362**, 219–223.
Romão, C. M., Louro, R., Timkovich, R., Lubben, M., Liu, M.-Y., Le Gall, J., Xavier, A. V. & Teixeira, M. (2000). *FEBS Lett.* **480**, 213–216.
Romão, C. M., Regalla, M., Xavier, A. V., Teixeira, M., Liu, M.-Y. & Le Gall, J. (2000). *Biochemistry*, **39**, 6841–6849.
Shukla, S. K. & Reed, K. D. (2000). *J. Clin. Microbiol.* **38**, 1701–1702.